Separation & Purification Reviews
Publication details, including instructions for authors and subscription information:
http://www.informaworld.com/smpp/title~content=t713597294

Zonal Centrifugation

H. W. Hsu[a]
[a] Department of Chemical and Metallurgical Engineering, The University of Tennessee, Knoxville, TN

To cite this Article Hsu, H. W.(1976) 'Zonal Centrifugation', Separation & Purification Reviews, 5: 1, 51 — 95
To link to this Article: DOI: 10.1080/03602547608066048
URL: http://dx.doi.org/10.1080/03602547608066048

SEPARATION AND PURIFICATION METHODS, 5(1), 51-95 (1976)

ZONAL CENTRIFUGATION

H. W. Hsu
Department of Chemical and Metallurgical Engineering
The University of Tennessee, Knoxville, TN 37916

Since the late Professor T. Svedberg began to apply centrifugal force for the study of colloid systems, progress in centrifugation has continued in two parallel directions. The first line of development has produced the analytical ultracentrifuge, which incorporates an optical system for the analysis of small amount of material while it is being centrifuged through a homogeneous medium (the solvent) under ideal conditions. The analytical centrifuge is now widely used not only to characterize molecular weight, but also to give insights into the size, shape, density and the base composition and activity of biopolymers and other macromolecules. The second line of development has produced the preparative centrifuge, which uses centrifugal force to sediment the solid phase of materials. The preparative centrifuge is a simpler instrument and does not have an optical system. However, recent rapid technical progress and development permit the preparative centrifuge not only to completely separate several or all of the components in a mixture, but also to perform analytical measurements. This versatile technique is known as density gradient centrifugation.

The density gradient method involves a supporting column of fluid whose density increases toward the bottom of the centrifugal tube. The density gradient fluid consists of a suitable low molecular weight solute in a solvent in which the sample particle

can be suspended. The extreme usefulness of swing-out rotors in density gradient work has been well proven. However, the relatively small volumes that can be handled in high centrifugal fields, together with the mechanical handling procedures; "wall effects" and "droplet sedimentation" etc. impose certain limitations on the technique and resolution. It was therefore necessary to design a rotor to eliminate these limitation, and the result was the series of zonal rotors produced at Oak Ridge National Laboratory by Anderson and co-workers [1].

Zonal Rotors

The only practical way to increase the quantity of sample handled in a density gradient solution is to increase the area of the sample cavity. The geometry of this requirement was found in a large cylindrical cavity rather than tubes. Cylindrical or bowl-shaped zonal rotors are now commonly used and are highly efficient tools for isolating and purifying a variety of particles of biological interests. The two important design features to note are: (i) the rotor itself is cylindrical and is divided internally by a series of radial septa (usually four), giving rise to sector-shaped cavities. The septa prevent, or at least minimize, turbulence when accelerating or decelerating. (ii) the detachable static seal assembly through which the density gradient and the sample are pumped into and out of the rotor while it is spinning. The rotor is normally loaded at low speed, and then the seal assembly is removed so that the centrifuge lid may be closed and the run up to high speed under vacuum (minimizing heating due to friction). Since the first zonal centrifuge rotor was built in 1954 by Anderson [2,3], over fifty different zonal centrifuge designs have been developed, constructed and evaluated. These have been grouped into a series of classes designed by letter with each design in a given class designated by a Roman numeral, followed in some instances by an indication of the material of construction. The following four rotor series are of general interest:

A series. Low-speed rotor for the separation of particles in the range of size visible in the light microscope (maximum speed of

6,000 rev/min, usually a fat-shaped, diameter of the rotor is much larger than the rotor height).

B series. Intermediate-speed rotors (up to 45,000 rev/min) for the separation of particles in the range of size visible in the electron microscope.

K series. Rotors and rotor systems for commercial vaccine production and protein purification (up to 35,000 rev/min for continuous-sample-flow-with banding).

J series. Small-scale K series for laboratory use (up to 100,000 rev/min).

The properties of a number of these rotors have been summarzied elsewhere by Anderson [4]. A partially assembled B-XV rotor, the completely assembled rotor with the removable upper seal in place are shown in Figs. 1 and 2 respectively. In Fig. 3 the rotor and

FIGURE 1

Partially assembled B-XV rotor.

FIGURE 2
Completely assembled B-XV rotor with removable upper seal in place.

seal in place in the Spinco Model L preparative Z-II centrifuge are shown. A side view of the assembled rotor in position in the centrifuge is presented in Fig. 4. Several schematic diagrams of operations that apply to B-XIV and B-XV zonal centrifuge rotors are shown in Fig. 5. The pertinent data on the B-XIV and B-XV rotors are shown in Table I.

In addition to speed advantages gained by titanium construction, rotors constructed of this material may be steam-sterilized and do not corrode in most salt solutions or at pH's used in biological studies. The suggested operating speeds which are maximum safe

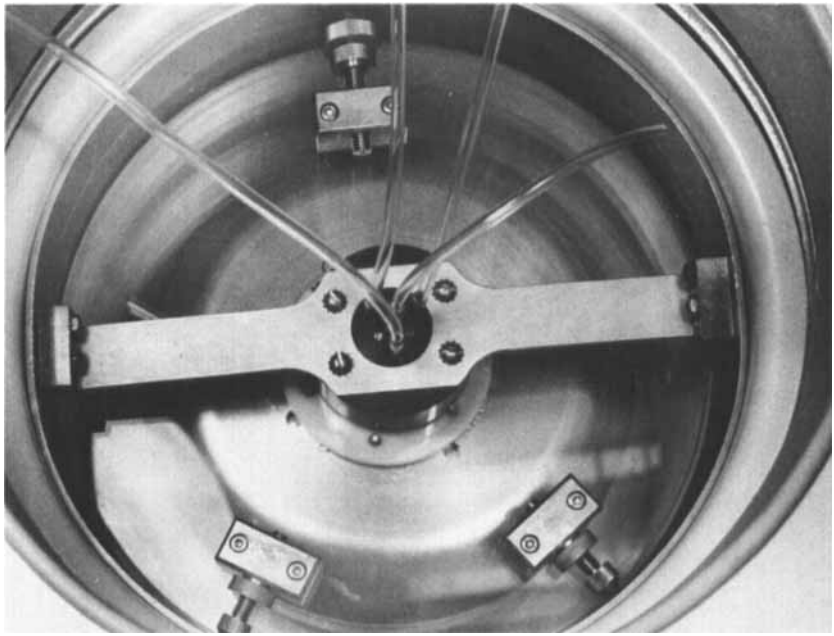

FIGURE 3

Rotor and Seal in place in Spinco Model L Z-II preparative ultracentrifuge.

speeds for B-XIV and B-XV rotors, as functions of the specific gravity of the fluid used, are shown in Fig. 6. Note that when a dense, homogenous fluid is centrifuged for a long period of time, a gradient is generally formed which will markedly increase the wall pressure in the rotor. For safe operation, the density of a gradient is considered as that of its densest portion. Those rotors were designed for research and were not for adaption to large-scale efforts. The K-series were developed for the purification of large quantities of virus and subcellular particles[6-9]. The techniques of continuous-sample-flow-with banding were also developed by Anderson and his co-workers at Oak Ridge National Laboratory [10-16]. A typical disassembled K-centrifuge rotor is presented in Fig. 7. A safe rotor chamber (armor

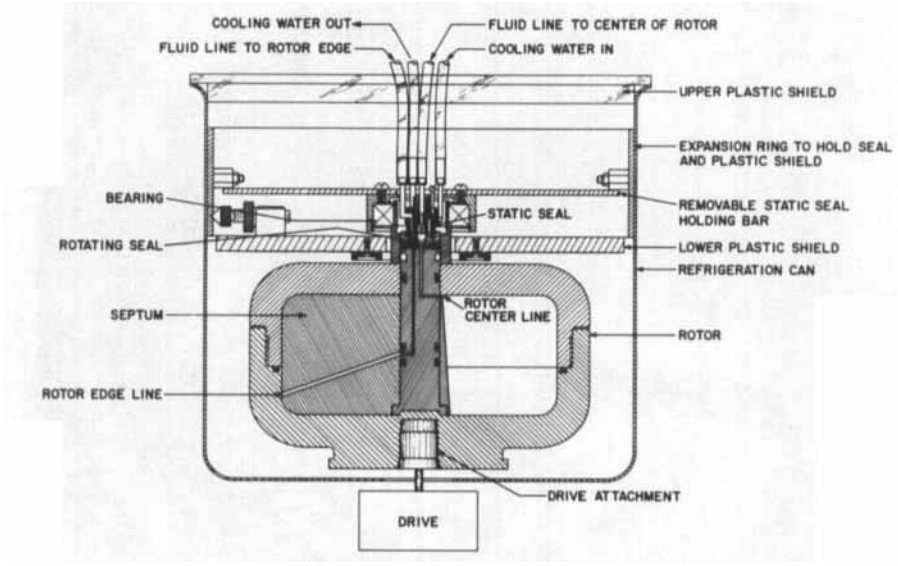

FIGURE 4

Side view of assembeld rotor in position in centrifuge during loading.

shielding) and the K-series centrifuge closed in an armor shielding ready for operation are shown in Figs. 8 and 9 respectively.

Effects of different numbers of septa on the shear-stress and velocity distributions of fluid during acceleration and deceleration have been investigated by Pham and Hsu [17]. In their investigation, profiles of two-dimensional velocity components; v_r, the radial velocity component, and v_θ, the tangential velocity component, and distributions of the radial shear stress, τ_{rr}, and the tangential shear stress, $\tau_{r\theta}$, in Beckman size B-XV zonal centrifuge rotors during acceleration and deceleration have been investigated by the method of birefringence using a milling yellow dye as an optical solution. The density-viscosity relationship of 1.2-2.0 wt % milling yellow aqueous solutions are very close to that of sucrose aqueous solutions at the same

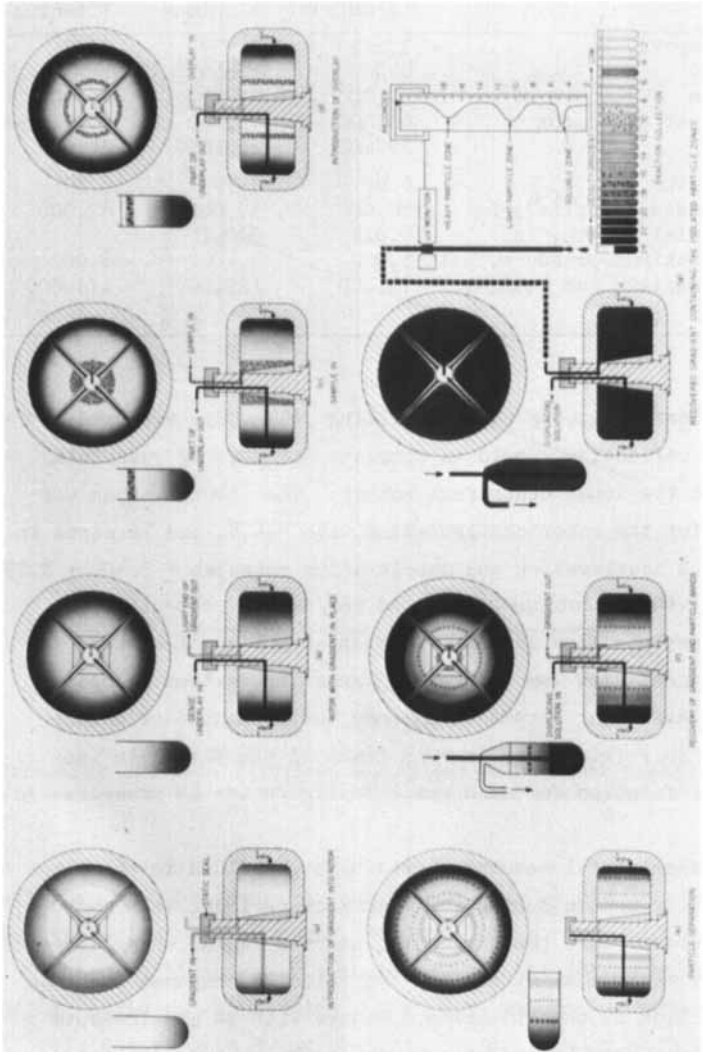

FIGURE 5

Schematic diagram of operation that apply to B-XV and B-XIV zonal centrifuge rotors.

TABLE I
Operating Data for B-XIV and B-XV Zonal Rotors (5)

Parameter	B-XIV (Aluminum)	B-XV Aluminum	B-XV Titanium
Weight (empty), kg	3,571	7,439	12.7
Volume, cc	649	1,666	
Speed, rpm	30,000	21,000	26,000
Maximum g, at rated rpm	60,000 at 29,400	45,000 at 21,5000	60,000 at 24,000
Maximum radius, cm	6.62	8.79	8.79
Maximum stress (tensile), psi	50,000	50,000	82,000
Maximum radial growth, in.	0.013	0.0175	
Estimated maximum pressure, psi	5,000	5,4000	8,000
Estimated maximum end load, lb	75,000	125,000	175,000

density. Therefore, the aqueous milling yellow dye was used as the double refraction liquid to simulate the density sustaining solution in the zonal centrifuge rotors. The investigation was performed for the rotor configuration with 3,4,6, and 12 septa in a rotor with acceleration and deceleration rates at $\pm$ 0.40, $\pm$ 0.75, $\pm$ 1.50, $\pm$ 3.00 revolutions per second per second respectively.

The complete flow field for instantaneous quasi-steady two-dimensional flow was obtained by relating various velocity components and shear stress components to the amount of double refraction (birefringence) in each frame of the film. An iso-stream line function for each rotor configuration is presented in Fig. 10.

The experimental results showed that the fluid in the rotor has a swirling motion during the transient periods; at reduced radius of about 0.62, the tangential and the radial shear stresses exhibit the maximum magnitude and the velocity components change their direction at that location. Rotors with 3- and 12-septa configurations show lower shear stresses than the other rotor configurations but have more prominent secondary flows. Rotors with 4- and 6-septa configurations exhibit no secondary flow

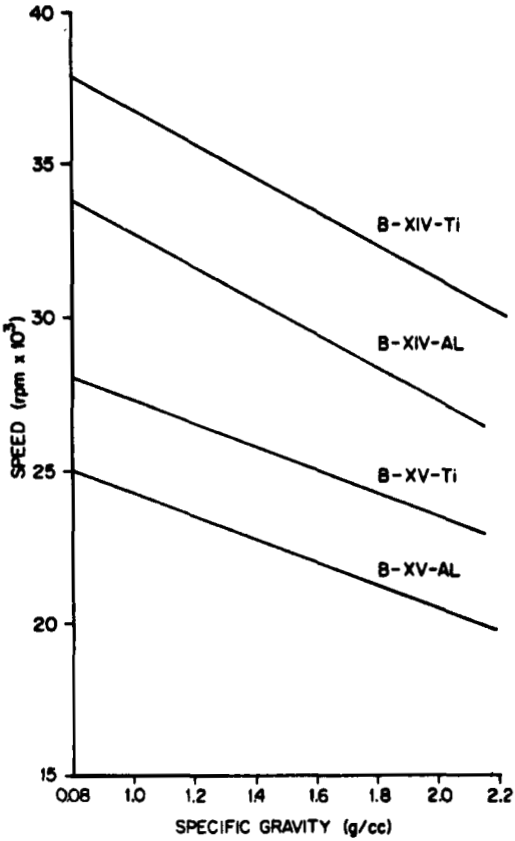

FIGURE 6

Operating Speed of Aluminum and Titanium B-XV and B-XIV rotors as a function of the density of the fluids in the rotor.

patterns, but the shear stresses are four to six times higher than those in 3- or 12-septa configuration rotors.

Based on these experimental results, the following rotor configuration is recommended for a given separation task.

1. Rotors with 3- or 12-septa configurations should be used for long, chained particle separation where low shear stresses are critical during the transient period.

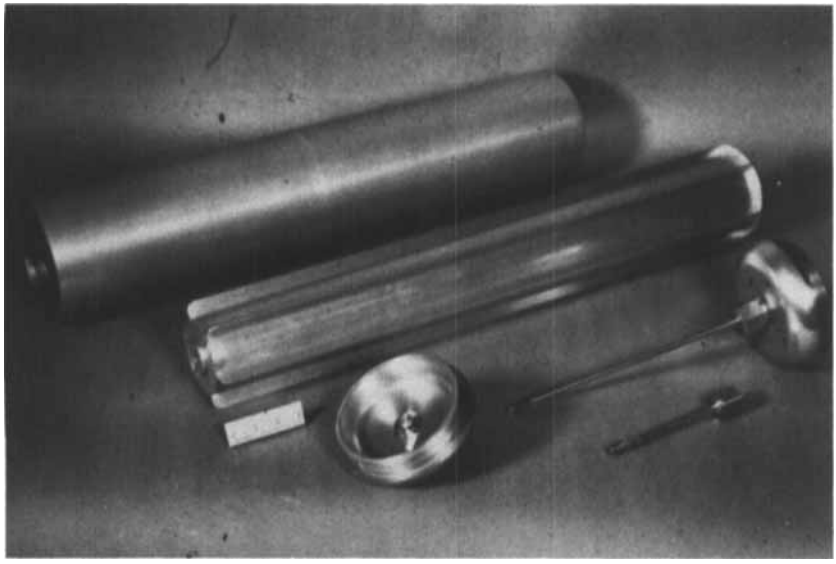

FIGURE 7

Disassembled K-type centrifuge rotor.

2. A rotor with a 4-septa configuration should be used for spherical particle separation where remixing due to secondary flows is critical during the transient period.

The experimental results also revealed that changing the rate of acceleration produces no noticeable effect in any flow patterns, shear stress distributions, or their magnitudes during each transient period. This is, coincidentally in agreement with the analysis of isodenisty paraboloid surface for reorienting gradient systems made by Hsu [18].

Dispersion in Zonal Gradient Centrufugation

The use of zonal centrifuges has two primary objectives:

(a) separation and purification of biological materials from sample mixture, and

(b) concentration of separated biological material from a dilute solution.

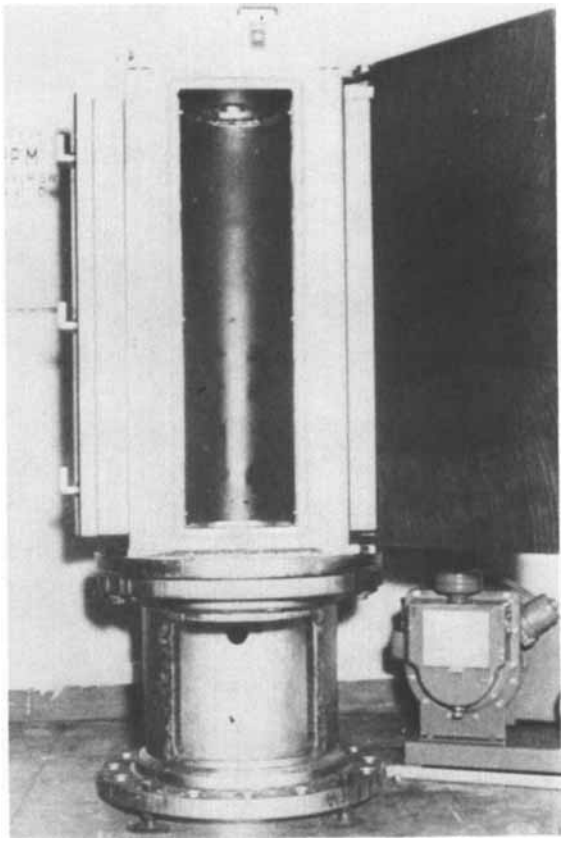

FIGURE 8

An armor shielding for K-rotor.

These two objectives are related. An optimum separation and purification is achieved by having a high resolution in each separated zone or band, and concentration increases as density of separated biological material in a band increases, likewise to achieve a high resolution in a separated zone. A band broadening effect in zonal centrifugation is due to a complicated phenomena of interaction of diffusion and sedimentation. Genung and Hsu [19]

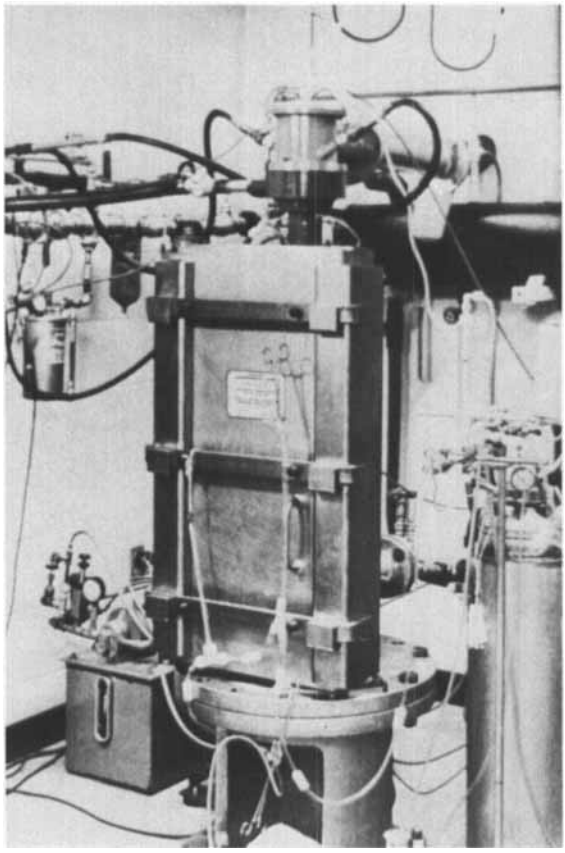

FIGURE 9

K-series rotor closed in an armor shielding ready for operation.

lumped all the contributing factors together and called them dispersion coefficient. In the determination of parameters which effect dispersion between sedimenting macromolecules and the sustaining gradient solution, dispersion coefficients of two sizes of polystyrene latex beads (diameters: 0.91 $\pm$ 0.0058 μ and 0.312 $\pm$ 0.0022 μ) and bovine serum albumin (BSA) in sucrose and Ficoll (polysucrose from Pharmacia Fine Chemicals, Sweden), 9.5 to 10% W/V step gradient and 10 to 25% W/V linear-with volume gradient

solutions, have been measured in an Oak Ridge B-XV zonal centrifuge rotor at 20°C at 2500 rpms for various times. Dispersion coefficients were obtained from experimental data on intensity of UV absorbance of macromolecule versus volume fractions using Schumaker's moment analysis formulae [20]

$$\frac{\langle r^2\rangle + 2D/s\omega^2}{\langle r^2\rangle_o + 2D/s\omega^2} = \exp\left[2\omega^2 s(t - t_o)\right] \tag{1}$$

$$\frac{\langle r^4\rangle - 2\langle r^2\rangle^2}{\langle r^4\rangle_o - 2\langle r^2\rangle_o^2} = \exp\left[4\omega^2 s\ (t - t_o)\right] \tag{2}$$

where the n-th moment of concentration i about the center of rotation is defined by

$$\langle r^n\rangle = \frac{\int_{r_1}^{r_2} r^n c_i r dr}{\int_{r_1}^{r_2} c_i\ r dr} \tag{3}$$

in which the quantities r_2 and r_1 are related to the bandwidth, which is a significant measure of resolution in a separation process. The sedimentation and dispersion coefficients were then obtained by simultaneous solution of Eqs. (1) and (2) together with the experimental data of r_1 and r_2 .

In order to make the experimental results general and more useful, dispersion coefficients were correlated in a dimensionless number, the Schmidt number ($S_c = \bar{\eta}/\bar{\rho}D$), as a function of various dimensionless parameters. Using results from step-gradient solution runs by a trial-and-error method, it is found that the following formula

$$Sc = 105[30F^{1.03}\ (Ta\cdot Q)^{-1} + 19\ Se^{0.19}\tau]^{1.02} \tag{4}$$

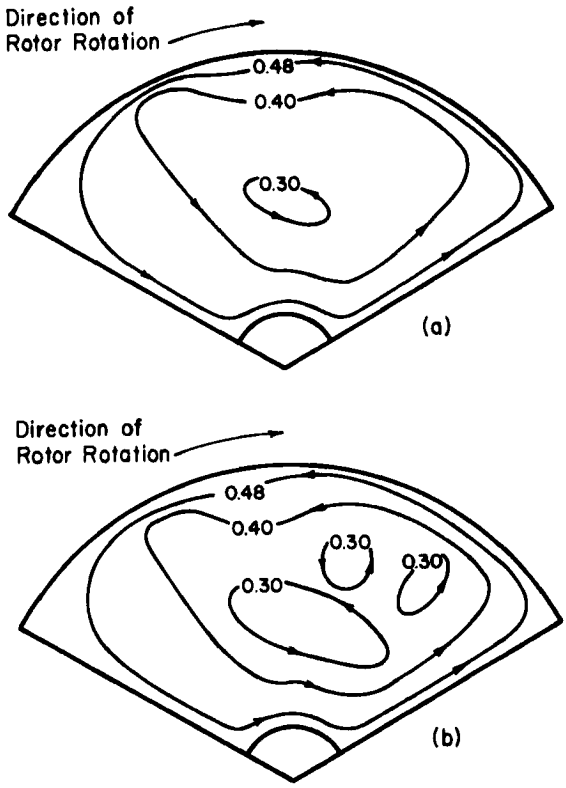

FIGURE 10

Transient flow patterns for 3-, 4-, 6-, 12-septa rotors at (a) 800 rpm and (b) 1800 rpm.

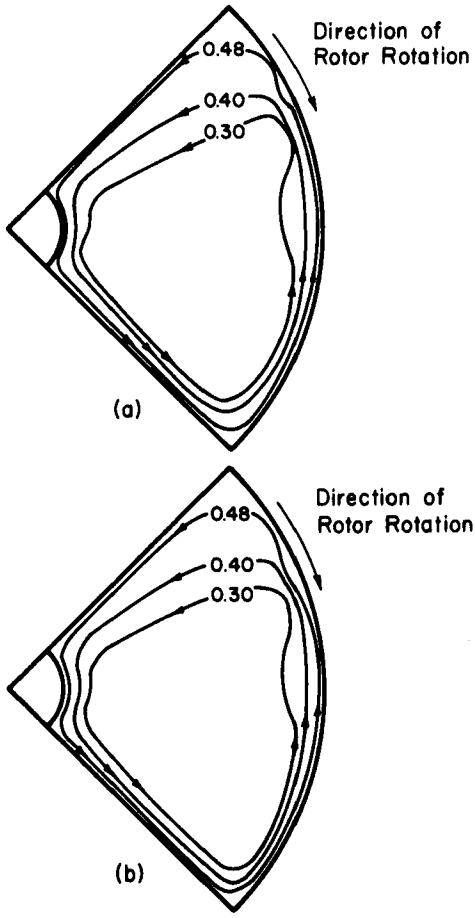

FIGURE 10 (continued)

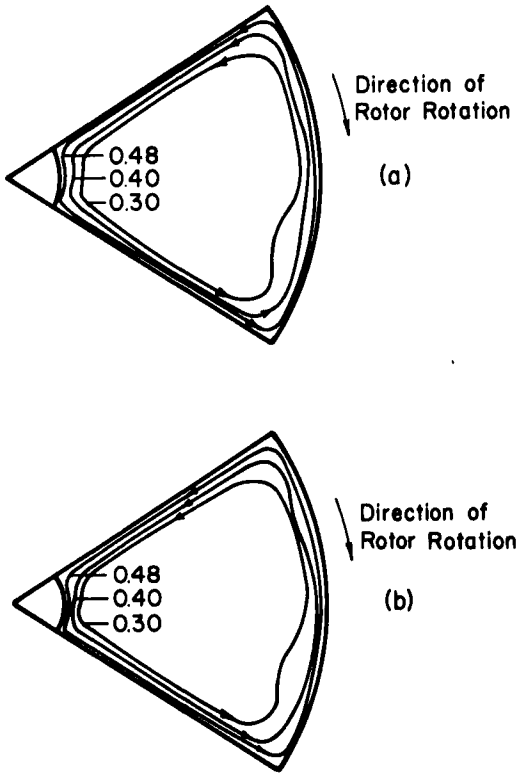

FIGURE 10 (continued)

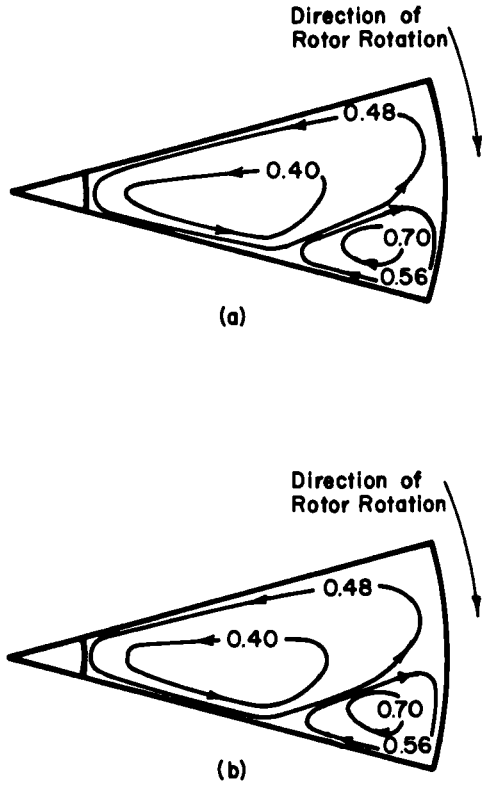

FIGURE 10 (continued)

fits all the data points within an average deviation of 2.5% and a maximum deviation of 6.3%. Various quantities in Eq. (4) are

$$Sc = \frac{\bar{\eta}}{\bar{\rho} D}$$ Schmidt number

$$F = \frac{\omega^2 t d_p^2 \bar{\rho}}{\bar{\eta}}$$ reduced centrifugal force field strength

$$Ta = \frac{\omega^2 d_p R \bar{\rho}}{\bar{\eta}}$$ Taylor number

$$Q = \rho_o / \rho_p$$ density ratio

$$Se = \frac{s \omega^2 R^2 \bar{\rho}}{\bar{\eta}}$$ reduced sedimentation coefficient

$$\tau = \frac{\bar{\eta} t}{\bar{\rho} R^2}$$ reduced time

The quantities $\bar{\eta}$ and $\bar{\rho}$ are viscosity and density of the gradient solution evaluated over the band-width values, η_o and ρ_o are the light end of viscosity and density of the gradient solution respectively. D is the dispersion coefficient between sample and a gradient solution, instead of the customary term of the diffusion coefficient. If $Q<1$, a sedimentation takes place until $Q = 1$ (isopycnic point).

The results obtained from the linear-with-volume gradient solution runs were checked against Eq. (4). A good agreement exists. All the data points were within an average of 3.5% deviation and a maximum of 8.9% deviation. They are assumed to be within the range of experimental errors, so that a further correlation to improve the results were not made. Equation (4) and both correlations from a step gradient solution and a linear-with-volume gradient solution are presented in Fig. 11.

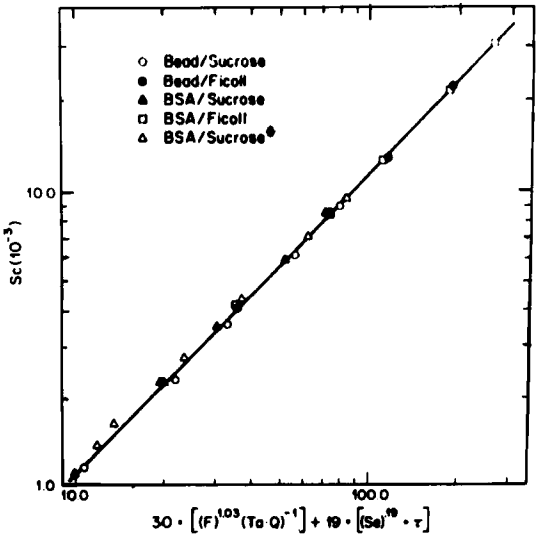

FIGURE 11

A plot of Eq. (4) and general correlation of experimental data points (*Runs whose data were not used in the correlation).

Equation (4) and Fig. 11 may be used to estimate a dispersion coefficient on new biomaterials for which sizes of particles and their sedimentation coefficients are available. The dispersion coefficient accounts for both eddy and molecular diffusions. It was observed that the dispersion process decreases exponentially until a considerable centrifation time and after this time the dispersion coefficient approaches to a constant value, a molecular diffusivity. Therefore, the eddy diffusion coefficient may be estimated by substracting the asymptotic constant from the observed dispersion coefficients. For a B-XV type rotor, the results are presented elsewhere [19].

Density Gradient Solutions

All centrifugation techniques depend on the shape of the gradient and on the gradient properties which are variable with respect to space coordinate, in terms of concentration. The

shape of the gradient is important in achieving the desired separation, and in determining properties such as buoyant density and sedimentation coefficient. In order to prescribe an exact profile of a density gradient solution at a given rotor location and at a specified time, one has to know the diffusivity of a gradient solute in a solvent as a function of its concentration which is a function of space coordinates.

There is no ideal all-purpose gradient material. A density gradient solution in zonal rotors is usually formed by a sucrose aqueous solution whose density and viscosity increase with distance from the axis. Cesium chloride aqueous solution is often used for isopycnic separations, because it has a relatively high density and low viscosity in the usual concentration range. Additional considerations in selecting a gradient material include the following [21]:

(1) Its density range should be sufficient to permit separation of the particles of interest by the chosen density gradient technique, without overstressing the rotor.

(2) It should not affect the biological activity of the sample.

(3) It should be neither hyperosmotic nor hypoosmotic when the sample is composed of sensitive organelles.

(4) It should not interfere with the assay technique.

(5) It should be removable from the purified product.

(6) It should not absorb in the ultraviolet or visible range.

(7) It should be inexpensive and readily available; more expensive materials should be recoverable for reuse.

(8) It should be sterilizable.

(9) It should not be corrosive to the rotor, particularly for zonal or continuous flow operation.

(10) It should not be flammable or toxic to the extent that its aerosols could be hazardous.

Table II lists some commonly used gradient materials, with their solvents and densities at 20°C. In order to prescribe more accurately a shape of a density gradient solution, concentration dependent binary diffusivities, viscosities, and densities of potassium citrate and potassium tartrate [22], Ficoll and methyl cellulose M-278 [23], and Sucrose and Sorbitol [24] have been measured by a microinterferometric method. The partial specific volume and the activity coefficient of those solutes were also obtained as functions of their respective solute concentrations.

This information is important, not only in prescribing the performed density gradient profile in a zonal rotor, but also in

TABLE II

Commonly Used Gradient Materials with Their Solvents [21]

Materials	Solvent	Maximum Density at 20°C
Sucrose (66%)	H_2O	1.32
Sucrose (65%)	D_2O	1.37
Silica sols	H_2O	1.30
Diodon	H_2O	1.37
Glycerol	H_2O	1.26
Cesium chloride	H_2O	1.91
	D_2O	1.98
Cesium formate	H_2O	2.10
Cesium acetate	H_2O	2.00
Rubidium chlordie	H_2O	1.49
Rubidium formate	H_2O	1.85
Rubidium bromide	H_2O	1.63
Potassium acetate	H_2O	1.41
Potassium formate	H_2O	1.57
	D_2O	1.63
Sodium formate	H_2O	1.32
	D_2O	1.40
Lithium bromide	H_2O	1.83
Lithium chloride	D_2O	1.33
Albumin	H_2O	1.35
Sorbitol	H_2O	1.39
Ficoll	H_2O	1.17
Metrizamide	H_2O	1.46

the prediction of self-forming gradient solutes in a zonal rotor by diffusion and sedimentation. The data points obtained from measurements are presented in Tables III and IV. The partial specific volume ν_o of water were determined graphically by the method of intercepts from the densities.

The quantity D_o in Table IV was obtained by extrapolation to an infinite diultion from a diffusivity vs. concentration plot. The activity coefficient was obtained from the equation given below (22)

$$\ln\gamma^{(c)} = \int_o^c \left[\frac{D\eta}{D_o\eta_o\nu_o\rho} - 1\right] d \ln c \qquad (5)$$

The quantities, D, ρ, ν_o, and η are all functions of concentration. Hence, substituting experimentally determined values of each quantity at various concentrations into the integrand and performing a numerical integration to that concentration, the activity coefficient at that concentration was obtained.

Empirical formulae for the diffusion coefficient and the activity coefficient as a function of the solute concentration were also obtained. They are listed below:

Potassium citrate:

$$D \times 10^6 = 2.305 + 10.986c - 30.080c^2 + 27.289c^3 \ (cm^2/sec); \quad (0.0556) \qquad (6)$$

$$\ln\gamma^{(c)} = 4.727c - 2.435c^2 + 16.942c^3 - 26.687c^4 + 19.326c^5 \qquad (7)$$

or

$$\ln\gamma^{(c)} = -0.31 + 1.91\left[0.37 + \frac{2.90c}{1.75 - 0179c}\right]^{1.35}; \ (0.0370) \qquad (7\text{-a})$$

in wt% of solute (w)

$$\ln\gamma^{(w)} = -0.31 + 1.91\left[0.31 + \frac{1.62w}{1 - w}\right]^{1.35} \qquad (7\text{-b})$$

TABLE III

Denisty, Viscosity, and Partial Specific Volume at 25°C at Various Concentrations

c (g-solute/ml)	η(centipoise)	ρ(g-solution/ml)	$\bar{v}_o$(ml/g-solution)
	Potassium Citrate		
0.1031	1.065	1.031	1.000
0.2207	1.383	1.104	1.000
0.3530	1.970	1.176	1.000
0.5045	3.496	1.260	0.955
0.6740	5.350	1.345	0.955
	Potassium Tartrate		
0.1038	1.022	1.039	1.000
0.2199	1.258	1.100	1.000
0.3546	1.695	1.182	0.969
0.5021	2.500	1.256	0.959
0.6701	4.280	1.340	0.959
	Ficoll		
0.050	11.8	1.013	1.010
0.075	12.6	1.021	1.010
0.100	13.2	1.028	1.010
0.220	18.0	1.059	1.010
0.310	23.0	1.077	1.010
0.400	28.0	1.096	1.010
0.550	41.0	1.119	1.010
0.700	60.0	1.139	1.010
	Methyl Cellulose		
0.050	1.78	1.012	1.001
0.075	6.15	1.017	1.001
0.100	17.89	1.022	1.001
0.125	56.38	1.028	1.001
0.150	158.45	1.034	1.001
0.175	500.00	--	--
0.200	1,690.00	2.136	1.001
	Sucrose		
0.3375	2.7384	1.1250	1.000
0.3944	3.5283	1.1464	0.999
0.4726	5.2199	1.1755	0.997
0.5473	7.9508	1.2055	0.994
0.6198	12.7500	1.2322	0.992

TABLE III Cont.,

c (g-solute/ml)	η(centipoise)	ρ(g-solution/ml)	$\bar{v}_o$ (ml/g-solution)
	Sorbitol		
0.1025	1.2290	1.0250	1.003
0.2120	1.8363	1.0600	1.003
0.3305	2.9397	1.1015	1.003
0.4544	4.6915	1.1360	1.003
0.5853	9.4778	1.1705	1.003

Potassium tartrate:

$$D \times 10^6 = 1.000 + 13.903c - 19.484c^2 + 16.785c^3 \ (cm^2/sec); \quad (0.0588) \qquad (8)$$

$$\ln\gamma^{(c)} = 13.903c - 6.827c^2 + 32.613c^3 - 28.398c^4 + 19.571c^5 \qquad (9)$$

$$\ln\gamma^{(c)} = 1.58\left[0.91 + \frac{4.82c}{1.75 - 0.79c}\right]^{1.64}; \ (0.1077) \qquad (9\text{-a})$$

in wt% of solute (w)

$$\ln\gamma^{(w)} = 1.58\left[0.91 + \frac{2.69w}{1 - w}\right]^{1.64}; \ (0.108) \qquad (9\text{-b})$$

Ficoll:

$$D \times 10^6 = 1.161 + 5.488C - 5.594c^2 + 9{,}949c^3 \ ; \ (0.195) \qquad (10)$$

$$\ln\gamma^{(c)} = 81.25C + 938.00c^2 - 3581.20c^3 + 5485.94c^4 - 2703.55c^5 \ ; \ (0.680) \qquad (11)$$

in wt % of solute (w)

$$\ln\gamma^{(w)} = 17.00\left[1.00 + \frac{0.50w}{1.00 - w}\right]^{7.36}; \ (1.67) \qquad (11\text{-a})$$

TABLE IV

Diffusion Coefficient and the Calculated Physcial Parameters at 25°C at Various Concentrations

C (g-solute/ml)	D x 10^6 (cm^2/sec)	$\eta/\eta_o\bar{\nu}_o\rho$	$\ln\gamma^{(c)}$
	Potassium Citrate (D_o x 10^6 = 2.305)		
0.1031	3.149	1.156	0.4774
0.2207	3.539	1.402	1.0536
0.3530	3.712	1.874	1.8022
0.5045	3.620	3.251	2.8449
0.6740	4.420	4.660	4.4540
	Potassium Tartrate (D_o x 10^6 = 1.000)		
0.1038	2.191	1.100	1.4029
0.2199	3.387	1.280	3.0175
0.3546	4.207	1.656	5.1823
0.5021	5.116	2.322	8.2074
0.6701	6.629	3.724	15.2857
	Ficoll (D_o x 10^6 = 1.161)		
0.100	1.586	0.0702	14.44
0.220	2.415	0.0524	36.59
0.310	2.660	0.0416	51.56
0.400	2.750	0.0349	66.13
0.550	4.390	0.0242	98.54
0.700	5.620	0.0169	150.93
	Methyl Cellulose (D_o x 10^6 = 1.161)		
0.075	0.1659	0.147	0.25 x 10^3
0.100	0.1769	0.115	1.00 x 10^3
0.125	0.1858	0.162 x 10^{-1}	2.50 x 10^3
0.150	0.2140	0.058 x 10^{-1}	6.00 x 10^3
0.175	0.2886	--	---
0.200	0.3630	0.112 x 10^{-2}	43.74 x 10^3
	Sucrose - 0.025M Sodium Phosphate Buffer (D_o x 10^6 = 5.266)		
0.3375	8.451	2.724	0.1309
0.3944	--	3.499	0.7946
0.4725	8.790	4.986	2.1232
0.5473	9.300	7.422	3.8938
0.6198	10.900	11.808	5.1377
	Sorbitol (D_o x 10^6 = 5.2659)		
0.1025	5.524	1.338	1.3421
0.2120	7.625	1.933	3.8064
0.3305	13.476	2.978	8.2943
0.4544	16.527	4.609	16.1080
0.5853	18.846	9.036	28.9975

Methyl cellulose

$$D \times 10^6 = 0.110 + 1.715C - 19.527C^2 + 86.851C^3; \quad (0.0124) \tag{12}$$

$$\ln\gamma^{(c)} = 10.75C + 168.97C^2 - 1153.33C^3 + 3015.750C^4; \quad (0.046) \tag{13}$$

in wt% of solute (w)

$$\ln\gamma^{(w)} = 0.10 + 640\left[1.00 + \frac{10.00w}{1.00 - w}\right]^{10.1}; \quad (0.597) \tag{13-a}$$

Sucrose - 0.025 M Sodium Phosphate Buffer:

$$D \times 10^6 = 5.2659 + 8.2675C \; ; \quad (0.4008) \tag{14}$$

$$\ln\gamma^{(c)} = -6.2787 + 12.1543C^2 + 22.5125C^3 \tag{15}$$

Sucrose - Distilled Water:

$$D \times 10^6 = 5.2659 - 9.0681C + 6.6518C^2 - 2.4550C^3; \quad (0.1351) \tag{16}$$

$$\ln\gamma^{(c)} = -9.7571C + 26.7647C^2 - 25.5977C^3 + 13.0724C^4 - 3.6839C^5 \tag{17}$$

Sorbitol - 0.010 M Sodium Phosphate Buffer:

$$D \times 10^6 = 2.8000 + 13.5397C - 19.7006\,C^2; \quad (0.6013) \tag{18}$$

$$\ln\gamma^{(c)} = 6.7665C + 1.1449C^2 + 6.6876\,C^3 + 40.6578C^4 - 47.3264C^5 \tag{19}$$

Sorbitol - 0.025 M Sodium Phosphate Buffer:

$$D \times 10^6 = 2.8000 + 11.5405C - 13.1166C^2 \; ; \quad (0.9484) \tag{20}$$

$$\ln\gamma^{(c)} = 6.0502C + 1.6321C^2 + 8.1993C^3 + 34.6545C^4 - 31.5098C^5 \tag{21}$$

Sorbitol - 0.050 M Sodium Phosphate Buffer:

$$D \times 10^6 = 2.8000 + 6.6653C - 8.9353C^2 \; ; \; (0.4349) \qquad (22)$$

$$\ln\gamma^{(c)} = 4.3090C + 0.6998C^2 + 9.1592\,C^3 + 20.0149C^4 - 21.4651C^5 \qquad (23)$$

Sorbitol - 0.100 M Sodium Phosphate Buffer:

$$D \times 10^6 = 2.8000 + 7.5500C - 10.3814C^2 \; ; \; (0.5065) \qquad (24)$$

$$\ln\gamma^{(c)} = 4.6250 + 0.7463C^2 + 8.8272C^3 + 22.6718C^4 - 24.9319C^5 \qquad (25)$$

Sorbitol - Distilled Water:

$$D \times 10^6 = 2.8000 + 20.8788C + 64.9780C^2 - 91.9200C^3 \; ; \; (0.7764) \qquad (26)$$

$$\ln\gamma^{(c)} = 9.3853C + 33.9806C^2 + 15.1881C^3 + 46.8682C^4 + 156.0958C^5 - 184.0151C^6 \qquad (27)$$

The experiments show that the diffusivities of sucrose in distilled water decrease with an increase in sucrose concentration and increase with an increase in sucrose concentration in a sodium phosphate buffer solution. The diffusivities of sorbitol in distilled water increase rather significantly with an increase in sorbitol concentration, however, less variation in diffusivities was observed as the sorbitol concentration varies in sodium phosphate buffer. This information may play some role in the explanation of membrane transport phenomena.

Particle Sedimentation in Gradient Solutions

In order to design experimental runs, one needs to know the exact positions of each particle as a function of time in a given gradient solution. Because zonal rotors are basically cylindrical pressure vessels, a direct measurement by an optical method is almost always impossible.
mathematical prediction.

The sedimentation of a particle which does not behave osmotically in a density gradient solution and does not interact with other particles or with the gradient solvent is a function of the following:

(1) the amount and the duration of the applied centrifugal force field, usually indicated by $\omega^2 t$,

(2) the density and viscosity of the gradient solution medium,

(3) the size, shape and density of the particles.

One may assume a gradient solution whose viscosity and density increase with distance r from the axis is expressed by the polynomials

$$\eta = \eta_o \left(1 + \sum_{i=1} \lambda'_i r^i\right) \qquad (28\text{-a})$$

$$\rho = \rho_o \left(1 + \sum_{i=1} \varepsilon'_i r^i\right) \qquad (28\text{-b})$$

where η_o and ρ_o are the light-end of viscosity and density respectively. The coefficients λ'_i and ε'_i are characteristic constants for viscosity and density profiles in a rotor as a gradient solution. Then, using the following reduced variables:

$$Q = \rho_o/\rho, \qquad N = (\rho_o \omega R d_p/\eta_o)^2, \qquad \zeta = r/R \qquad (29\text{-a,b,c})$$

$$\tau = \eta_o t/\rho_o R^2, \qquad \lambda_i = \lambda'_i/R^i, \qquad \varepsilon_i = \varepsilon'_i/R^i \qquad (29\text{-d,e,f})$$

$$A = \left[\frac{1}{Q} - 1\right] \frac{N}{18} \cdot \tau = \text{(reduced time)} \qquad (29\text{-g})$$

into the sedimentation equation of a particle in an incompressible gradient solution relative to the rotating coordinate system[25,26]

$$\frac{dV_{ri}}{dt} + \frac{18\eta(r)}{\rho_i d_i^2} V_{ri} = \frac{\omega^2 r}{\rho_i} [\rho_i - \rho(r)]; \quad (i=1,2,\ldots,N) \qquad (30)$$

together with Eqs. (28) by a perturbation method for a boundary condition at

$$A = 0 , \zeta = \zeta_c \text{ (reduced rotor core edge position)} \qquad (31)$$

The quantities $\eta(r)$ and $\rho(r)$ are the viscosity and density of the gradient solute as a function of radial distance from the rotating axis, which are the characteristics of a gradient solution, Eqs. (28). ρ_i and d_i are the i-th particle's density and size respectively and V_{ri} is the sedimentation velocity of the i-th particle. In the derivation of Eq. (30), the particles are all assumed to be spherical and drag force on the particles during the sedimentation can be approximated by Stokes's resistance law. For the non-spherical particles, the equation can be modified by the introduction of appropriate shape correction factors in the usual fashion. Since time is measured from the instant of band formation, the axial velocity component V_z and the anglar velocity component V_θ were not considered. The term "particle" is used to cover dissolved substances and particles of both microscopic and macroscopic dimensions, i.e., everything except the suspending fluid, which is usually water.

Mathematical expressions for

(a) a particle position as a function of reduced rotation time,

(b) an instantaneous particle sedimentation coefficient in a given gradient solution,

(c) the shear-stress exerted by a particle during zonal centrifugation runs in a given gradient solution

have been obtained by Hsu [26].

The mathematical expressions were also tested with the zonal experimental data, numbers 813 and 859 at the Molecular Anatomy Program, Oak Ridge National Laboratory, rat serum sedimenting through 10-25% sucrose gradient in a B-XIV rotor. The mathematical prediction of a particle's position in a rotor for a given

rotation time agrees excellently with experiments for both runs. It is anticipated that these expressions will be widely used in conducting zonal centrifugation runs and in design of zonal experiments.

In using those expressions, the characteristic constants, λ_i and ε_i, of gradient solutions have to be determined by fitting into the forms given in Eqs. (28), which can be done easily with accuracy by a computer.

Optimal Density Gradient Profile for Sedimentation-Velocity Method

The sedimenation velocity mehtod is a transport method. The solute particles are forced to settle at appreciable rates toward the wall of the rotor by application of a high centrifugal force. The local viscosity of a density gradient solution is the major factor in controlling the rate of particle movement[26]. The ability to design an optimal density gradient solution and to estimate when and where the best separation is taking place, so that one can stop the centrifugation run and collect the separated fractions from a rotor before particles reach their respective isopycnic points, is of primal importance in the sedimentation-velocity method.

Recently, Hsu[27] has used Pontryagin's maximum principle[28] to obtain

(a) the optimal profile of a density gradient solution characterized by viscosity and density profiles which are expressed as function of the radial distance of a zonal rotor,

(b) the estimation of an optimal centrifugation time, so that the resolution of separation by the sedimentation-velocity method will be maximum,

(c) the predication of each particle's position at the optimal centrifugation time.

The mathematical derivation is briefly presented below for a sedimentation-velocity separation. A performance index for the separation between particle 1 and particle 2 is defined by

$$\text{Max } [\Delta R = \int_0^{t_f} (\frac{dr_1}{dt} - \frac{dr_2}{dt})\ dt] \qquad (32)$$

in which r_1 and r_2 are the instantaneous positions of particles 1 and 2 and can be taken as center of mass of bands containing particles 1 and 2. The problem was formulated to seek a density gradient solution characterized by a viscosity profile, $\eta(r)$, and a density profile, $\rho(r)$, which maximizes the difference of instantaneous band positions of two particles in a rotor, and that maximizes the resolution of a separation at the final time, t_f. The constraint conditions associated with the performance index, Eq. (32), are given by a multicomponent Lamm equation [29] (the continuity equations for centrifugation in a cylindrical rotor relating the change of concentration with time to the divergence of the flow of solute particles to sedimentation and diffusion, for particle 1 and particle 2) together with the definition of sedimentation velocity.

$$\frac{dr_1}{dt} = \frac{k_1\omega^2 r}{\eta(r)} \cdot \frac{\rho_1 - \rho(r)}{\rho_1 - \rho(H_2O,20°C)} \qquad (33\text{-a})$$

$$\frac{dr_2}{dt} = \frac{k_2\omega^2 r}{\eta(r)} \cdot \frac{\rho_2 - \rho(r)}{\rho_2 - \rho(H_2O,20°C)} \qquad (33\text{-b})$$

Equations (33a,b) are obtained by combining the definition of sedimentation coefficient of Svedberg [30,31] and then converting the instantaneous sedimentation coefficient to the standard sedimentation coefficient in 20°C water medium. The quantity k_i is defined as

$$k_i = s_i^\circ\ (H_2O,\ 20°C) \cdot \eta(H_2O,\ 20°C) = \text{const.} \qquad (33\text{-c})$$

The boundary conditions for the properties of the light-end density gradient solution at the rotor core, r_c, are

$$\rho(r_c) = \rho_o \tag{34-a}$$

$$\eta(r_c) = \eta_o \tag{34-b}$$

The optimal viscosity profile obtained by the maximum principle is

$$\eta(r) = \eta_o \left(\frac{r}{r_c}\right)^{4/3} \tag{35-a}$$

The optimal density profile is obtained by using the boundary condition, Eq. (34a) together with Eq. (35a), which gives

$$\rho(r) = (\rho_o - \alpha) \left(\frac{r}{r_c}\right)^{2/3} + \alpha \tag{35-b}$$

in which

$$\alpha = \frac{1 - \left(\frac{\rho_2}{\rho_1}\right)\left(\frac{s_2^o}{s_1^o}\right)\left(\frac{\rho_1 - \rho_H}{\rho_2 - \rho_H}\right)}{1 - \left(\frac{s_2^o}{s_1^o}\right)\left(\frac{\rho_1 - \rho_H}{\rho_2 - \rho_H}\right)} \quad ; \text{ where } \rho_H = \rho(H_2O,\ 20°C) \tag{35-c}$$

The final positions of particles 1 and 2 are then obtained from the Euler-Lagrange equations for the multiplier functions $\lambda_3[t_f] = \lambda_4[t_f] = 0$ (detail in Ref. [28]) as the conditions for the Pontryagin maximum principle. They are:

$$r_1(t_f) = r_c \left\{ \frac{\frac{4}{6}\left[\frac{s_1^o(\rho_1 - \alpha)}{\rho_1 - \rho_H} - \frac{s_2^o(\rho_2 - \alpha)}{\rho_2 - \rho_H}\right] + \frac{s_1^o(\rho_2 - \rho_1)}{\rho_1 - \rho_H}}{\left[\frac{k_1}{\rho_1 - \rho_H} - \frac{k_2}{\rho_2 - \rho_H}\right] \cdot (\rho_o - \alpha)} \right\}^{\frac{3}{2}} \tag{36-a}$$

$$r_2(t_f) = r_c\left\{\frac{-\frac{4}{6}\left[\frac{s_1^o(\rho_1-\alpha)}{\rho_1-\rho_H}-\frac{s_2^o(\rho_2-\alpha)}{\rho_2-\rho_H}\right]+\frac{s_2^o(\rho_2-\rho_1)}{\rho_2-\rho_H}}{\left[\frac{s_1^o}{\rho_1-\rho_H}-\frac{s_2^o}{\rho_2-\rho_H}\right]\cdot(\rho_o-\alpha)}\right\}^{\frac{3}{2}} \qquad (36\text{-b})$$

The maximum separation ΔR is obtained by the difference between Equations (34a) and (34b), which is then given by

$$(\Delta R)_{max} = r_c\left\{\frac{\frac{4}{3}\left[\frac{s_1^o(\rho_1-\alpha)}{\rho_1-\rho_H}-\frac{s_2^o(\rho_2-\alpha)}{\rho_2-\rho_H}\right]}{\left(\frac{s_1^o}{\rho_1-\rho_H}-\frac{s_2^o}{\rho_2-\rho_H}\right)\cdot(\rho_o-\alpha)}+\frac{(\rho_2-\rho_1)}{(\rho_o-\alpha)}\right\}^{\frac{3}{2}} \qquad (37)$$

An optimal centrifugation time is then obtained using Equation (33a) and (34a) together. The result in a reduced form is:

$$\tau_f = \frac{1}{A\cdot B}\sum_{n=0}^{\infty}\frac{3M^n}{2(n+2)}\cdot\zeta_c^{\frac{2(n+2)}{3}}\left[\left\{\frac{\frac{4}{6}\left[\frac{k_1(\rho_1-\alpha)}{\rho_1-\rho_H}-\frac{k_2(\rho_2-\alpha)}{\rho_2-\rho_H}\right]+\frac{k_1(\rho_2-\rho_1)}{\rho_1-\rho_H}}{\left[\frac{k_1}{\rho_1-\rho_H}-\frac{k_2}{\rho_2-\rho_H}\right]\cdot(\rho_o-\alpha)}\right\}^{n+2}-1\right] \qquad (38)$$

in which

$$\tau = \frac{\eta_o t}{\rho_o R^2}, \quad S_i = \frac{s_i^o\omega^2R^2{}_o}{\eta_o}, \quad \beta_i = \frac{\rho_i}{\rho_o}, \quad \delta = \frac{\eta(H_2O,20^oC)}{\eta_o} \qquad (39\text{-a,b,c,d})$$

$$A = \frac{S_i \cdot \delta}{\beta_i - \beta_H}, \quad B = \beta_i - \alpha, \quad c = \frac{1-\alpha}{\zeta_c^{2/3}}, \quad M = c/B \qquad (39\text{-e,f,g,h})$$

An interesting result is that all the diffusion coefficients in Lamm's equation cancel out and do not show up in the expressions obtained. This may be due to the fact that in velocity-sedimentation, the centrifugation time is generally very short. Therefore, concentrations of macromolecular particles and a density gradient solution do not disperse appreciably and are offset by sedimentation velocity

Stability Analysis of Isopycnic Banding

The separation of biological material in a zonal centrifugation frequently uses the equilibrium method. As the banding particles move outward from the axis with velocity V_r and reach their respective zones of isodensity in the sustaining gradient solution, V_r vanishes and equilibrium state (isopycnic banding), is established. Being able to maintain stable zones of banding particles is of importance since an understanding of this may lead to an estimate of the maximum amount of particles that can be loaded into a given density gradient without the loss of resolution during the banding of the particle zones. A complete understanding of factors which affect stable isodenisty banding would also lead to specification of the best set of operating conditions and the composition of gradient solutions for any separation task.

Previous work in this area is sparse and limited in scope. Unstable phenomena during band centrifugation have been observed by Anderson [32] and Brakke [33,34]. A quantitative experimental study of this instability has been done by Nason, et al.[35] In order to explain this instability Svensson et al.[36] and Schumaker [20] have assumed that instability is due to the formation of a density inversion within the fluid by diffusion. In studying this turnover effect, Sartory [37] has used a small linear perturbation analysis to determine whether the disturbance grows or

decays in time for two layers of stationary diffusing solute in a common solvent in a graditational field. His theory predicts that instability occurs under the much wider range of conditions $\bar{\rho}_2^o / \bar{\rho}_1^o > (D_2/D_1)^{3/2}$ for sufficiently long times with thick upper layers, and under conditions $\bar{\rho}_2^o / \bar{\rho}_1^o > (D_2/D_1)^{5/2}$ for sufficiently long times with very thin upper layers. The quantities $\bar{\rho}_2^o$ and $\bar{\rho}_1^o$ are initial macromolecular (particle) density and initial salt density respectively. D_2 and D_1 are diffusivities of macromolecules in a gradient medium and in a gradient medium with salt. Halsall and Schumaker [38] have conducted experiments to determine the onset of turnover effect in diffusion experiments in zonal centrifuge. They found that the stability criterion for their experiment is $\bar{\rho}_2^o/\bar{\rho}_1^o < (D_2/D_1)^{1.010}$. They concluded that their discrepancy from Sartory's prediction may be due to inhomogeneity or association-dissociation of the sample under study. Meuwissen and Heirwegh [39] have shown experimentally that the stability of zones in liquid density gradients under a normal gravitational field depends on the strength of the supporting gradient.

Hsu [40] has made an analysis for stability of isopycnic banding in zonal centrifugation. Due to the isopycnic condition, the analysis can be made by the lumped parameter method and an analytical solution can be obtained. The result is summarized in the following.

A small perturbation analysis has been applied to the generalized Lamm sedimentation equation [29] to determine whether the disturbance grows or decays in time for two stationary diffusing solutes [a gradient solute (1) and a macromolecule (2)] in a solvent (0) in a given centrifugal force field. The criterion for the stability has been obtained in terms of normal modes, so that the perturbations decay with time. It is found that the stability criterion is given by

$$\alpha r \leq \left\{ 1 - \frac{(D_{11} + D_{22})^2}{D_{11}D_{22} - D_{12}D_{21}} \left[\frac{D_{11} + D_{12}}{(D_{11} + D_{22})^2} \cdot \frac{\omega^2 d_2 r^2 \bar{\rho}_2}{18\eta} \cdot \left(3 - \frac{d \ln \eta}{d \ln r}\right) + \frac{1}{4} \left(1 - \frac{1}{D_{11} + D_{22}} \cdot \frac{\omega^2 d_2^2 r^2 \bar{\rho}_2}{18\eta}\right)\right] \right\}^{\frac{1}{2}} \quad (40)$$

It is implied that the stability of isopycnic banding is determined by the band-width (αr), the maximum band capacity as the right-hand of the equation.

The stability criterion given in the equation presents the unifying theroy. The theory obtained from the previous observations during centrifugation, such as density inversion theory, and the theory from the infinitesimal perturbation analysis of diffusional phenomena under one gravitational field are inclusively represented.

It is interesting to note that Meuwissen and Heirwegh's conclusion,[39] the stability depends on the shape or strength of the supporting gradient, is also represented by the terms of $(3 - \frac{d \ln \eta}{d \ln r})$ and $\frac{\omega^2 d_2 r^2 \rho_2}{18\eta}$ in Equation (40). If the gradient increases with cube of radius, the term $(3 - \frac{d \ln \eta}{d \ln r})$ drops out. The shape of gradient is not a factor for the stability. If the slope of a gradient viscosity is $\frac{d \ln \eta}{d \ln r} > 3$, the contribution of that term to the stability is negative, thus the maximum load capacity is reduced. If $(\frac{d \ln \eta}{d \ln r}) > 3$ the steeper the gradient solution the more the stability of a system. In this case, the band-width increase with the slope of a gradient solution; thus the range of the stable region increases. The same conclusion can also be drawn for the density inversion theory. If the shape of a gradient is $(\frac{d \ln \eta}{d \ln r}) > 3$, the second term at the right hand side of Equation (40) is positive. Therefore,

the following situation has occurred in the gradient, $\bar{\rho}_2 < \bar{\rho}_{grad} \cdot (3 - \frac{d \ln \eta}{d \ln r}) > 3$, since at an isopycnic point $\bar{\rho}_2 = \bar{\rho}_{grad}$. Thus density inversion does take place in order to return to the physical stable situation. If $(\frac{d \ln \eta}{d \ln r}) > 3$, i.e., $\bar{\rho}_2 > \bar{\rho}_{grad} \cdot (3 - \frac{d \ln \eta}{d \ln r})$, the system remains unchanged within the region. If a system is under one gravitational field, i.e., the terms containing $\omega^2 d_2^2 \bar{\rho}_2/18\eta$ drop out, the stability criterion becomes

$$\alpha r \geq \sqrt{1 - \frac{(D_{-1} + D_{22})^2}{4(D_{11}D_{22} - D_{12}D_{21})}} \tag{41}$$

The criterion is similar to that obtained by Sartory [37] except for the powers on the diffusivities. The four diffusivities for three component systems can be obtained by Fujita and Gosting's procedure [41].

An additional characteristic besides previous theories, which appears in Equation (40) is that one would like to increase the right hand side of Equation (40) so that the stability range can be increased. In order to increase the right hand side of Equation (40) for a given system, one will set the term

$$\frac{\omega^2 d_2^2 r^2 \bar{\rho}_2}{(D_{11} + D_{22})\eta} < 1$$

After rearranging, it becomes

$$\omega < \frac{1}{d_2 r} \left[\frac{(D_{11} + D_{22})\eta}{\bar{\rho}_2} \right]^{1/2} \tag{42}$$

in which r is the position where ideal isopycnic banding takes place. Equation (42) shows that the increasing of angular velocity in a zonal run does not improve the resolution. The angular velocity has to be constrained by Equation (42). The physical interpretation of this phenomena is that with too high

angular velocity, the banding solute penetrates too deep into a gradient solution, therefore an instability due to a density inversion or lack of strength in a supporting gradient will take place. Therefore, the angular velocity also has to be constrained.

The stability criterion is such a complicated phenomenon that one should consider all possible means to increase the right hand side of Equation (40). Thus, Equation (40) shows the unification of all previous theories.

A Special Application of Zonal Centrifuge

Zonal centrifugation in a large cylindrical rotor has been developed as a general method for the mass separation and purification of a wide variety of biological materials ranging in size from whole cells to protein molecules. Applications of zonal centrifuges are now so numerous that it is no longer possible to servey and abstract all the applications in this article. It is only possible to report a few special applications of density gradient techniques.

The sedimentation rate of a biological substance, its banding density or both of these properties can be altered by attaching a biological substance to a neutral carrier substance. Since the pioneering work of Singer and Plotz [42] who utilized the prinicples of particulate clumping during antigen-antibody interactions to develop clinical detection techniques for rheumatoid factor (RF), an appreciable number of works have appeared dealing with the particulate carrier reactions in serology [43-45]. The procedures employed consist, in general, of coating the carrier particules with a suitable antigen or antibody, and using these coated hybrid particules to detect antibody or antigen in sera or other fluids. Density gradient centrifugation allowed an accurate determination of the agglutination reaction. If the volume and density of the carrier of a hybrid are known, then the positive or negative other load (biological substance) may be determined from the buoyant density of the hybrid. If the buoyant density of the load

is known, then its volume and hence its mass, can be calculated [45].

The buoyant density of a hybrid particle is given by the formula:

$$\rho_H = \frac{V_c\rho_c + V_L\rho_L}{V_c + V_L} \qquad (43)$$

where V and ρ are volume and density, and subscripts H, C, and L refer to hybride, carrier, and load respectively. Equation (43) may be rearranged to give an expression for the mass of the load:

$$M_L = \frac{V_c(\rho_H - \rho_c)}{1 - \rho_H/\rho_L} \qquad (44)$$

All quantities in the right-hand side of Eq. (44) are known except the density of the hybride, which is to be determined by the centrifugation against a density gradient by separation and isopycnic banding. Since the mass of an individual antigen or antibody molecule in the hybrid can be determined, the number of molecules attached to the neutral carrier particules can also be determined.

Using the technique described above Genung and Hsu [46] have determined adsorption isotherms of four antigens on polystyrene latex particules (diameter of 0.109 ± 0.0025 μ) and also studied the interaction of antigen coated hybrid latex spheres with their specific antibodies. Based on the technique of density gradient centrifugation, the reaction mass can be accurately determined, the mechanism of antigen-antibody interactions were modeled. Using a similar technique. Cohen and Mire [47] have studied enzyme-substrate interactions and Sethy and Cullinan [48] studied thermodynamic behavior of the system aceton-carbontetrachloride.

Discussion

Preparative zonal centrifugation is now in a state of very rapid growth, with new rotor systems and separative techniques

appearing at frequent intervals. The evaluation of these methods and comparison with other methods in a variety of specific instances will require a period of several years.

We conclude that rotor development should proceed in those directions:

(1) The limits of speed, capacity, volume and resolution should continue to be explored using systems which exhaust presently available technology.

(2) The improvement of zonal centrifugation should be directed to an improvement in loading and unloading methods to reduce the dispersion caused by these operations. So that the separated resolution may be adequately maintained during the unloading.

(3) An optimal design for rotor configuration is required for a particular separation. Transport phenomena of particles in a rotor with respect various configuration have to be studied in detail, so that various factors affecting separation in a rotor can be evaluated quantitatively.

Acknowledgements

The author wishes to express his sincere appreciation to Dr. N. G. Anderson for introducing the zonal centrifugal separation techniques to the author and for his constant encouragement and many constructive discussions while he was at Oak Ridge National Laboratory as Director of the Molecular Anatomy Program. The partial financial support of a NSF Grant, ENG 72-04241-A01 is gratefully acknowledged. Many of figures presented here were made at Oak Ridge National Laboratory. The author is also very grateful for the permission to reuse them in this review article.

References

1. N. G. Anderson, "The Development of Zonal Centrifuges and Ancillary System for Tissue Fractionation and Analysis," Natn. Cancer Inst. Monogr. 21, (1966).
2. N. G. Anderson, Semi-annual Report, USAEC, ORNL-1953 (1955).
3. N. G. Anderson, Bull. Am. Phys. Soc. I (2), 267 (1956).

4. N. G. Anderson, Quart. Review Biophys. I (3), 217 (1968).
5. N. G. Anderson, D. A. Walter, W. D. Fisher, G. B. Cline, C. E. Nunley, and C. T. Rankin, Analyt. Biochem. 21, 235 (1967).
6. N. G. Anderson, D. A., Walter, C. E. Nunley, R. F. Gibson, R. M. Schilling, E. C. Denny, G. B. Cline, E. F. Babelay, and T. E. Perardi, Analyt. Biochem. 32, 460 (1969).
7. T. E. Perardi, R. A. A. Leffler, and N. G. Anderson, Analyt. Biochem. 32, 495 (1969).
8. T. E. Perardi and N. G. Anderson, Analyt. Biochem. 34, 112 (1970).
9. J. N. Brantley, D. D. Willis, J. P. Breillatt, R. E. Gibson, L. C. Patrick, and N. G. Anderson, Analyt. Biochem. 36, 434 (1970).
10. N. G. Anderson, Nature, 199, 116 (1963).
11. N. G. Anderson, C. L. Burger, and H. P. Barringer, Federation Proc. 23 , 140 (1964).
12. H. P. Barringer, N. G. Anderson, and C. E. Nunley, in "The Development of Zonal Centrifuges and Ancillary Systems for Tissue Fractimation and Analysis," edited by N. G. Anderson, Natn. Cancer Inst. Monogr., 21, 191 (1966).
13. N. G. Anderson, H. P. Barringer, J. W. Amburgey, Jr., G. B. Cline, C. E. Nunley, and A. S. Berman, in "The Development of Zonal Centrifuge and Ancillary Systems for Tissue Fractimation and Analysis," edited by N. G. Anderson, Natn. Cancer Inst. Monogr., 21, 199 (1966).
14. C. B. Cline, C. E. Nunley, and N. G. Anderson, Nature 212, 487 (1966).
15. N. G. Anderson, in "Method of Biochemical Analysis," edited by D. Glick, Vol. XV, Interscience (Wiley), New York, 1967, p. 271.
16. N. G. Anderson and G. B. Cline, in "Methods in Virology," edited by K. Maramorosch and H. Hoprowski, Vol. II, Academic Press, New York, (1967), p. 137.

17. H. D. Pham and H. W. Hsu, I & E C Process Design & Develop., 11, 556 (1972).
18. H. W. Hsu, Separ. Sci., 8 (5), 537 (1973).
19. R. K. Genung and H. W. Hsu, Separ. Sci., 7 (3), 249 (1972).
20. V. N. Schumaker, in "Advances in Biological and Medical Physics," edited by C. A. Tobins and J. H. Lawrence, Vol. II, Academic Press, New York, 1967, p. 245.
21. O. M. Griffith, "Technique of Preparative Zonal, and Continuous Flow Ultracentrifugation," Beckman Instruments, Inc., April, 1975.
22. D. M. McDonald and H. W. Hsu, Separ. Sci., 7 (5), 491 (1972).
23. L. R. Bell and H. W. Hus, Separ. Sci., 9 (5), 401 (1974).
24. V. S. Shah and H. W. Hsu, Separ. Sci., 10 (6), 787 (1975).
25. H. W. Hsu, J. Chinese Inst. Chem. Engr. 1, 1 (1970).
26. H. W. Hsu, Separ. Sci., 6 (5) , 699 (1971).
27. H. W. Hsu, Math. Biosci, 23, 179 (1975).
28. R. E. Kopp, in "Optimization techniques," edited by G. Leitmann, Acad. Press, New York, 1962.
29. H. Fujita, "Mathematical Theory of Sedimentation Analysis," Acad. Press, New York, 1962.
30. T. Svedberg, Z. Phys. Chem. 127, 51 (1927).
31. T. Svedberg and K. O. Pederson, "The Ultracentrifuge," Oxford Univ. Press. London, 1940.
32. N. G.Anderson, Exptl. Cell. Res., 9 446 (1955).
33. M. K. Brakke, Arch. Biochem. Biophys., 55, 175 (1955).
34. M. K. Brakke, Advances Virus Res., 8, 193 (1960).
35. P. Nason, V. N. Schumaker, H. B. Halsall, and J. Schwedes, Biopolymers, 7, 247 (1969).
36. H. Svensson, L. Hagdahl, and K. D. Lerner, Sci. Tvols., 4, 1 247 (1969).
37. W. K. Sartory, Biopolymers, 7, 251 (1969).
38. H. B. Halsall, V. N. Schumaker, Biochem. and Biophys. Res. Communica. 43, 601 (1971).

39. J. A. T. P. Meuwissen and K. P. N. Heirweigh, Biochem. and Biophys. Res. Communica. 41 657 (1970).
40. H. W. Hsu, Math. Biosci., 13, 361 (1972).
41. H. Fujita and L. J. Grosting, J. Phys. Chem., 64, 1256 (1960).
42. J. M. Singer and C. M. Plotz, Am. J. Med., 21, 888 (1956).
43. I. Oreskes and J. M. Singer, J. Immunology, 86, 338 (1961).
44. E. M. Ball and M. K. Brakke, Virology, 39, 746 (1969).
45. N. G. Anderson, J. P. Broillatt, Nature, (New Biology), 231, 114 (1971).
46. R. K. Genung and H. W. Hsu, a manuscript in preparation.
47. R. Cohen and M. Mire, Europ. J. Biochem., 23, 267 (1971).
48. A. Setby and H. T. Cullinan, Jr., AIChE J. 18, 829 (1972).

Nomenclature

A : parameter defined in Eq. (29-g) and in Eq. (39-e)
B : parameter defined in Eq. (39-f)
C : parameter defined in Eq. (39-g)
c_i : concentration of chemical species i
d_p : size of particle
D_{ij} : dispersion coefficient
D : multicomponent diffusivity
F : reduced centrifugal force field $[=\omega^2 t\bar{\rho}\ d_p/\bar{\eta}\ ]$
i : index for summation
k : parameter defined in Eq. (33-c)
m : parameter defined in Eq. (39-h) and in Eq. (44)
n : index for moment
N : parameter defined in Eq. (29-b)
Q : density ratio $[=\rho_o/\rho_p]$
r : radial variable
R : radius of centrifugal rotor or radial distance
s : Svedberg's sedimentation coefficient $[=dr/dt/\omega^2 r\ ]$
S_c : Schmidt number $[=\bar{\eta}\ /\bar{\rho}\ D]$
Se : reduced sedimentation coefficient $[=s\omega^2\bar{\rho}\ R^2/\bar{\eta}\ ]$
t : time variable

T : Taylor number $[=\omega^2 d_p R\bar{\rho}/\bar{\eta}\ ]$

v : velocity

w : weight percent

α : wave number, a real constant used in Eq. (40) or parameter defined in Eq. (35-c)

β : parameter defined in Eq. (39c)

$\tilde{\nu}_i$: partial specific volume of chemical species i

γ : activity coefficient

ρ : density

λ_i, λ'_i : characteristic coefficient for gradient viscosity variations

η : dynamic viscosity

δ : parameter defined in Eq. (39-d)

τ : reduced time $[=\bar{\eta}\ t/\bar{\rho}\ R^2]$

τ : shear stress

$\varepsilon_i, \varepsilon'_i$: characteristic coefficients for gradient density variations

ω : angular velocity

ζ : reduced radial variable defined in Eq. (29-c)

subscript

c : rotor core edge position or carrier

f : final condition

H : water, hybrid

i : particle of species i

L : load

o : average property of gradient fluid, solvent or water, or zero time as measured reference

p : particle

r : radial direction

z : axial direction

θ : tangential direction

superscript

o : condition of 20°C in water medium

Special symbols

< > : moment

(r) : function of(radial)variable

Δ : difference

- : average quantity